SUPPLEMENTARY INFORMATION

Active expiration induced by excitation of ventral medulla in adult anesthetized rats

Silvia Pagliardini, Wiktor A. Janczewski, Wenbin Tan, Clayton T. Dickson, Karl Deisseroth, Jack L. Feldman

SUPPLEMENTAL RESULTS

Phase Reset analysis

Although reset to a narrow induced phase range was a robust phenomenon, we did note that the phase at which stimulation was delivered had a modest effect on the induced phase. To more systematically assess this, we examined the relationship between stimulation phase and the subsequent induced phase (**Fig. S1**). Although reset occurred across all stimulation phases, as shown by the lack of convergence to the expected phase values, the onset of subsequent inspiration showed an increased delay at certain phases of respiration. At its maximum, this delay corresponded to a doubling of the lowest phase reset values (in this example from ~90° to ~180°). These increased delays were initiated in the period just after the peak of inspiratory flow and continued until the end of expiratory flow (**Fig. S1**). These results were a consistent feature across all experiments (n=7).

This phase dependence of rhythm reset by photostimulation led us to assess whether peak ∫EMGs also showed a similar relationship. We measured both the delay to onset and peak $\int ABD_{EMG}$ and $\int DIA_{EMG}$ evoked by photostimulation. While the delay to onset of activity showed a phase dependence similar to the effect on inspiratory flow onset (becoming longer in the period described above; **Fig. S1**), the peak amplitude of ∫EMGs were unrelated to the phase of respiration at which stimulation was delivered.

SUPPLEMENTAL LEGENDS

Fig. S1. Phase timing of brief photostimulation of SYN-ChR2-EYFP transfected RTN/pFRG neurons affects reset of respiratory cycle. Average respiratory flow (top), distribution of induced phase together with expected phase of respiration in the absence of a reset effect shown in blue (middle), and onset of DIA_{EMG} (empty circles) and ABD_{EMG} (filled circles) activity (bottom) are all shown with respect to the stimulus phase. A delay in the onset of the reset effect can be seen in each measure during the passive expiratory period.

Fig. S2. Results summary. Diagrams of serial transverse sections of the ventral brainstem at -11.30, -11.60 and -11.80 mm distances from bregma that depict the identified chemosensitive region of the RTN (summary of data obtained in several previous studies, (Mulkey et al., 2004; Guyenet et al., 2005; Stornetta et al., 2006; Abbott et al., 2009b)) and the region targeted in the present study. **A**) The gray area on the ventral surface of the brainstem represents the area where chemosensitive neurons have been identified by means of neuronal recordings and Phox2b immunoreactivity in prior work. **B**) Summary of the locations of the BIC/STRY injections (red arrow), the presumptive site of drug action (light red circle) and the location of the juxtacellularly recorded recorded neurons (black dots). **C**) Summary of the location of the viral injection (green arrow), the location of maximal response to laser stimulation and the presumptive location of the recorded neurons (green circles). Note the limited overlap between the region of interest in our study and the proposed RTN chemosensitive region depicted in **A**.

Figure S1

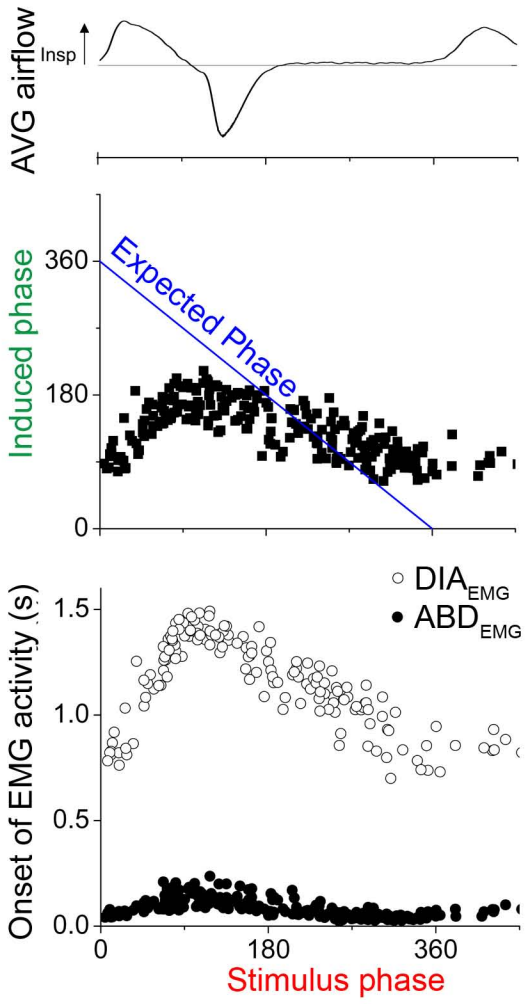
AVG airflow
Insp
Induced phase
360
180
0
Expected Phase
DIA EMG
ABD EMG
Onset of EMG activity (s)
1.5
1.0
0.5
0.0
0
180
360
Stimulus phase

Figure S2

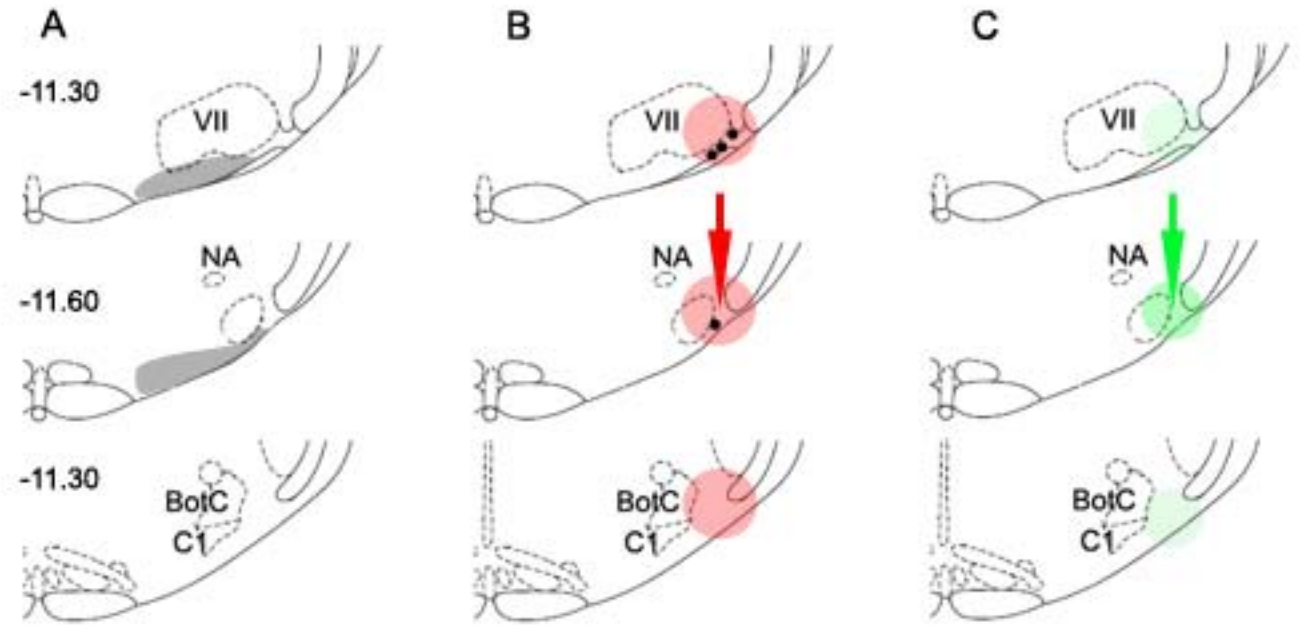

RTN CHEMOSENSITIVE REGION

BIC/STRY INJECTIONS AND RECORDING SITES

SYN EYFP CHR INJECTIONS AND STIMULATION SITES